Desalination and Water Treatment
www.deswater.com
doi: 10.1080/19443994.2014.923207

54 (2015) 3646–3653
June

Taylor & Francis
Taylor & Francis Group

Photocatalytic degradation of 4-chlorophenol using a $Ag/TiO_2/Fe_3O_4$ composite under UV-A irradiation

S.W. Chang[a,*], W.J. Chung[a], S.H. Yu[b], S.J. Lee[c]

[a]*Department of Environmental Energy Engineering, Kyonggi University, Iui-dong, Yeongtong-gu, Suwon-si, Gyeonggi-do, Republic of Korea, Tel. +82 31 249 9739; Fax: +82 31 254 4905; email: swchang@kgu.ac.kr (S.W. Chang)*
[b]*Advanced Radiation Technology Institute, Korea Atomic Energy Research Institute, Jeongeup, Jeonbuk, Republic of Korea*
[c]*Korea Environment Corporation, Environment Research Complex, Gyeongseo-dong, Seo gu, Incheon, Republic of Korea*

Received 15 January 2014; Accepted 14 March 2014

ABSTRACT

4-Chlorophenol (4-CP), widely used in the production of dyes, drugs, and fungicides is a water pollutant. It can be found in surface water, soil, ecosystems, and the human body. 4-CP is a non-degradable pollutant when subjected to traditional water treatment techniques. The development of advanced oxidation processes provided alternative methods that could potentially be applied to the decomposition of non-degradable compounds; 4-CP could then be removed from water supplies by processes such as photocatalytic degradation. However, the anatase TiO_2 typically used in such procedures has a large band gap of 3.2 eV which is only activated by ultraviolet (UV) radiation. In this study, a $Ag/TiO_2/Fe_3O_4$ composite was synthesized from Ag, TiO_2, and Fe_3O_4 owing to the enhanced photocatalytic activity and catalyst recoverability conferred by Ag and Fe_3O_4, respectively. The catalyst was characterized by X-ray diffraction, X-ray fluorescence, UV–visible spectrophotometry, scanning electron microscopy, transmission electron microscopy, diffuse reflectance spectroscopy, and energy dispersive spectroscopy. The catalyst surface appeared to be composed of small, spherical or ovoid particles with dimensions smaller than 50 nm. The synthesized catalyst showed much higher activity for the photodegradation of 4-CP than Degussa P25 TiO_2 and Ag/TiO_2 under UV-A irradiation. The *Langmuir–Hinshelwood* kinetic mechanism was used to compare the photocatalytic activities of Degussa P25 TiO_2, Ag/TiO_2, and $Ag/TiO_2/Fe_3O_4$.

Keywords: 4-Chlorophenol; $Ag/TiO_2/Fe_3O_4$; Photocatalytic degradation; *Lanmuir–hinshelwood*

1. Introduction

Chlorophenols (CPs) have been reported as toxic chlorinated pollutants by the US Environmental Protection Agency [1]. Most derivatives are difficult to degrade, toxic, and are bio-refractory in the natural environment. They have been widely used as paint, pesticide, and leather preservatives [2], Wagner and Nicell [3], and as a result of such processes, CPs are found in soil, groundwater, and surface water [1].

The degradation of phenolic compounds in wastewater is performed by techniques including biological

*Corresponding author.

Presented at the 5th IWA-ASPIRE Conference 8–12 September 2013, Daejeon, Korea

methods and chlorination. However, biological methods usually require lengthy treatment times, and toxic substances can harm the activity of the bacteria. The use of chlorination methods generates undesirable carcinogenic by-products [4].

Advanced oxidation processes (AOPs) are alternative methods to those described above for the decomposition of phenolic compounds (and other organics) in water [5]. Photocatalysis mediated by pure TiO_2 has allowed the development of AOPs, which can be conveniently applied to phenolic compounds in water [6]. However, pure TiO_2, which possesses a band gap of 3.0–3.2 eV, is inactivated by irradiation under visible light [7]. To mitigate this problem, pure TiO_2 has been modified by the incorporation of noble metals such as platinum, palladium, and silver (Fujishima and Honda [8], thus decreasing the band gap of TiO_2, and increasing the visible light absorption, owing to the presence of noble metals [9].

Chengzhu et al. [10] have reported the preparation of Ag/AgBr plasmonic photocatalysts through ion exchange and photoreduction methods, and the reaction showed highly efficient photocatalytic activity via irradiation with visible light. Wang et al. [11] have prepared AgI/TiO_2 by a deposition–precipitation method, which showed high efficiency for the degradation of non-biodegradable azo dyes under visible light irradiation. TiO_2@$ZnIn_2S_4$ composites promote the degradation of methylene blue under visible light irradiation [12]. Shi et al. [13] recently investigated the photocatalytic activity of P-doped TiO_2, which extended the spectrum of TiO_2 into the visible-light range.

Magnetic separation exhibits excellent ability of catalyst removal with many practical advantages including low cost, low toxicity, and ease of operation (Yavuz et al. [14]; synthetic TiO_2-magnetic composites could be an alternative method to facilitate the reuse of a catalyst [15]. Song and Gao [16] recently reported $TiO_2/SiO_2/Fe_3O_4$ magnetic spheres as easily recovered photocatalysts for the degradation of methylene blue [16,17]. Liu et al. [18] have reported the preparation of Fe_3O_4/CdS nanocomposites via a sonochemical route in an aqueous solution, which showed high photocatalytic activity toward the photodegradation of methyl orange [18,19].

The objective of this study was to improve the photocatalytic activity of $Ag/TiO_2/Fe_3O_4$ composite material. The photocatalyst was activated under UV-A irradiation. Using an external magnetic field, the catalyst could then be easily recycled without significant decrease in the photocatalytic activity. The *Langmuir–Hinshelwood* kinetic mechanism was used to compare the photocatalytic activity of Degussa P25 TiO_2 with Ag/TiO_2 and $Ag/TiO_2/Fe_3O_4$ respectively.

2. Experimental methods

2.1. Chemicals and materials

All chemicals used were of the highest purity. TiO_2 powder with an average particle size of 30 nm and surface area of 50 $m^2 g^{-1}$ was purchased from Degussa AG Company (P25 grade). Silver nitrate ($AgNO_3$), D-glucose, sodium dodecyl sulfate (SDS), hexadecyltrimethylammonium bromide (CTAB, $C_{16}H_{33}N(CH_3)_3Br$, >99.0% purity), 1-pentanol, ferric chloride ($FeCl_3$), and 4-CP (>99% purity) were purchased from Sigma-Aldrich. Ferrous sulfate ($FeSO_4{\cdot}7H_2O$), sodium hydroxide (NaOH), ammonia (28–30%, w/w, aqueous solution), ethyl alcohol (94.5%), and nitric acid (68–70%) were obtained from Samchun Pure Chemical Reagent Co. Ltd. Hexane (95%) was purchased from J.T. Baker. Deionized water was used for all synthetic procedures.

2.1.1. Synthesis of Ag nanoparticles

Silver nitrate (5.1 g) was dissolved in distilled water (500 mL). Aqueous ammonia (1.0 M) was added dropwise to the $AgNO_3$ solution with vigorous stirring until a colorless solution was obtained. This was followed by the addition of glucose (100 mL of a 0.1 M solution), SDS (50 mL of a 0.2 M solution), and distilled water (75 mL). Sodium hydroxide solution was added to adjust the pH to 11.5. The reaction was allowed to proceed for 10 min. The Ag nanoparticles were used for subsequent experiments without any additional purification.

2.1.2. Synthesis of Ag/TiO_2 nanoparticles

The Ag nanoparticles (0.1 g) prepared above were rinsed three times with ethanol, and then resuspended in ethanol (20 mL) under sonication for 2 h. The Ag nanoparticles were then resuspended in distilled water (100 mL), and the mixture was acidified with HCl (0.5 M, 1.10 mL). The Ag/TiO_2 nanoparticles were prepared from Ag nanoparticles in w/o micro-emulsions consisting of CTAB as the surfactant, 1-pentanol as the co-surfactant, and hexane as the oil phase. In a typical experimental procedure, the micro-emulsion solution was prepared by dissolving CTAB (1.0 g) in hexane (15 mL) and 1-pentanol (1 mL), which were stirred vigorously for 30 min until it became clear and transparent. TiO_2 (5 g) was then added to the above

micro-emulsion solution and sonicated for 30 min. The reaction was allowed to magnetically stir for 10 h. The resulting precipitated Ag/TiO_2 nanoparticles were separated by centrifugation, dried in air at 100°C for 24 h, and further calcined in air at 300°C for 2 h.

2.1.3. Synthesis of $Ag/TiO_2/Fe_3O_4$ composite

Fe_3O_4 nanoparticles (synthesized by the reaction between $FeSO_4{\cdot}7H_2O$ (9.34 g, 14 mmol) and $FeCl_3$ (7.8 g, 28 mmol) in the presence of ammonium hydroxide (100 mL, 5 mol L^{-1})) were added to the above micro-emulsion solution and sonicated for 30 min. Aqueous HNO_3 solution (2.0 mol L^{-1}) was then added to adjust the pH of the micro-emulsion solution until the pH was ca. 5–6, whereupon the Ag/TiO_2 nanoparticles (5 g) were added to the above micro-emulsion solution and sonicated for 30 min. The reaction was left to stir for 10 h. The resulting precipitated $Ag/TiO_2/Fe_3O_4$ nanoparticles were separated by centrifugation, dried in air at 100°C for 24 h, and further calcined in air at 300°C for 2 h.

2.2. Characterization of the $Ag/TiO_2/Fe_3O_4$ catalyst

Morphology observations were carried out using a SUPRA 55VP field emission scanning electron microscope (SEM, Carl Zeiss, Germany) and a JEM 2100F transmission electron microscope (TEM, JEOL, USA). The energy dispersive X-ray spectrometry technique was used to determine the elemental composition in the samples. X-ray diffraction (XRD) patterns, obtained on a D8 Advance instrument (Bruker, Germany) using Cu-Kα1 radiation at a scan rate (2θ) of 0.02° were used to determine the identity of any phases present. The X-ray fluorescence (XRF) experiments were performed using an S4 PIONEER instrument (Bruker, Germany). The light absorption properties of TiO_2, Ag/TiO_2, and $Ag/TiO_2/Fe_3O_4$ were studied by diffuse reflectance spectroscopy (DRS). DRS spectra were recorded on a DRA-2500 spectrometer (VARIAN, Germany) equipped with an integrating sphere. The spectra were recorded in diffuse reflectance mode and transformed to a magnitude F(R1), proportional to the extinction coefficient (k) via the Kubelka–Munk theory. Band-gap energy values were estimated from the plots of the modified Kubelka–Munk function vs. the energy of the excitation light, assuming anatase TiO_2 catalysts as indirect semiconductors: ([F(R∞)E]1/2).

2.3. Procedure of photocatalytic experiments

The photocatalytic activity of the prepared catalysts under UV-C and UV-A light was estimated by measuring the degradation rate of 4-CP in aqueous phase. The concentration of 4-CP was determined by an UV–visible spectrophotometer (DR5000, HACH, USA) according to its absorbance at 283 nm.

2.4. Effects of various parameters (dose, initial concentration, intensity)

Experiments were carried out using a stirred quartz reactor and a 6, 18, and 30 W UV lamp with UV irradiation peaks of 254 and 365 nm at an ambient temperature of about 20°C; 0.3, 0.5, and 0.7 g of the photocatalysts were added with stirring into 1,000 mL of aqueous 4-CP, of which the initial concentrations were 10, 20, and 30 mg L^{-1}, respectively. Samples of the suspension were withdrawn after a defined time interval and filtered through a 0.20 μm syringe filter. The filtered samples were analyzed for residual 4-CP concentration using a UV–visible spectrophotometer. The photocatalytic activity of the TiO_2, Ag/TiO_2, and $Ag/TiO_2/Fe_3O_4$ powders were also evaluated for comparative purposes. The cyclic experiments were carried out to determine the durability of 4-CP degradation by the $Ag/TiO_2/Fe_3O_4$ composite. Each sample was used repeatedly and each cycle lasted for 150 min. Before the beginning of the next cycle, the remaining solution was replaced with 20 mg L^{-1} of fresh 4-CP solution.

2.5. Kinetic studies

The photodegradation kinetics of 4-CP can be described by a modified *Langmuir–Hinshelwood* model, according to Eq. (1) [20].

$$r = -\frac{dc}{dt} = k_r\theta = \frac{k_r + Kc}{1 + Kc} \tag{1}$$

where k_r is the reaction rate constant, θ is the fraction of the surface covered by 4-CP, K is the adsorption coefficient of 4-CP, and c is the concentration of the solute. For very low concentrations of 4-CP (Kc1), we can neglect Kc in the denominator. Integration of Eq. (1) yields Eq. (2) with k as an apparent first-order rate constant.

$$\ln\frac{c_0}{c} = kt + a \tag{2}$$

3. Results and discussion

3.1. Characterization of the $Ag/TiO_2/Fe_3O_4$ composite

The structural characterization of the $Ag/TiO_2/Fe_3O_4$ composite was confirmed by XRD analysis

(Fig. 1). It was found that all the major diffraction peaks were perfectly indexed with the anatase phase of TiO_2. The generation of Fe_2O_3 must be avoided during the synthesis of Fe_3O_4, as Fe_2O_3 tends to interfere with the target experiment. The $FeTiO_3$, which is usually formed during the plasma-sprayed TiO_2/Fe_3O_4 coating at high temperature, was observed in this study. The use of sonication, instead of a motor-driven blade for stirring during $Ag/TiO_2/Fe_3O_4$ composite synthesis may be the reason.

The peaks assigned to Ag in non-calcined powder at $2\theta = 38.1^\circ$ and $2\theta = 64.4^\circ$, suggest successful reduction of Ag metal at TiO_2 surfaces. The results demonstrate the coexistence of silver, anatase TiO_2, and magnetic phases in the final products, and are in close agreement with other reported results.

XRF spectroscopy analysis of Ag/TiO_2 and $Ag/TiO_2/Fe_3O_4$ are presented in Fig. 2, from which the contained quantity of Ag/TiO_2 and $Ag/TiO_2/Fe_3O_4$ was calculated. The TiO_2 was calculated as ~97.6% in Ag/TiO_2, which therefore also contained about 2.4% of Ag. The proportion of Fe_3O_4 was calculated as about 50.6%, which therefore also contained 48.2% of TiO_2 and 1.2% Ag.

The diffuse reflectance spectra (DRS) of the catalyst samples Ag/TiO_2 and $Ag/TiO_2/Fe_3O_4$ are shown in Fig. 3. A plot of the modified Kubelka–Munk function vs. the energy of exciting light affords band-gap energies of 1.12 eV, 2.88 eV, and 3.12 eV for Degussa P25 TiO_2, Ag/TiO_2, and $Ag/TiO_2/Fe_3O_4$, respectively.

To explore the photocatalytic activities of the $Ag/TiO_2/Fe_3O_4$ (calcined at 300°C for 1 h), the degradation efficiencies of 4-CP (155.57 μmol L^{-1}) under UV-C and

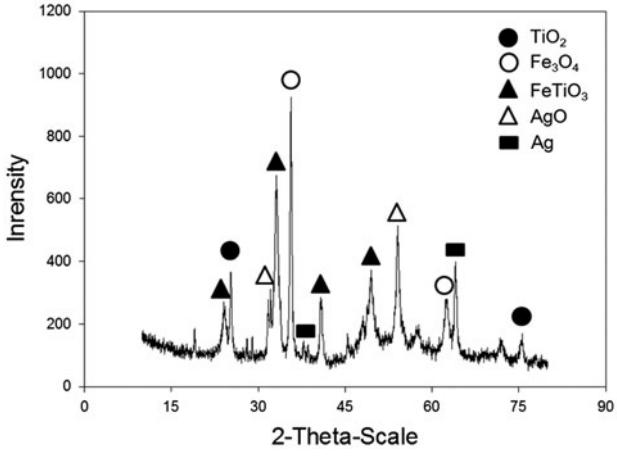

Fig. 1. XRD spectra of $Ag/TiO_2/Fe_3O_4$ particles.

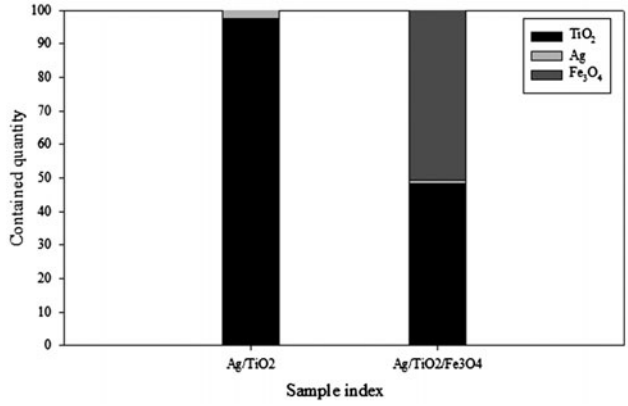

Fig. 2. Contained quantity of Ag/TiO_2 and $Ag/TiO_2/Fe_3O_4$ samples as determined by XRF analysis of photocatalytic degradation of 4-CP.

UV-A light irradiation sources were studied. Fig. 4 shows the degradation rate of 4-CP as UV-C (254 nm) and UV-A (365 nm). Using the Degussa P25 TiO_2 and $Ag/TiO_2/Fe_3O_4$ catalysts the concentration of 4-CP (as measured by the chemical oxygen demand) decreased by 69.4 and 82.13%, respectively (UV-C) and by 75.2 and 83.12%, respectively (UV-A).

The UV-A conditions exhibited a much higher degradation concentration of 4-CP than UV-C, due to the intense absorption of the lower band-gap energy of the $Ag/TiO_2/Fe_3O_4$ composite, which is illustrated in Fig. 3.

The effects of catalyst dose, initial concentration, and irradiation intensity were investigated to compare the 4-CP degradation. The first factor studied was an initial 4-CP concentration of 77.8, 155.6, and 233.4 μmol L^{-1}, respectively. The second factor was a dosage of $Ag/TiO_2/Fe_3O_4$ of 0.3, 0.5, and 0.7 g L^{-1}, respectively. The third factor was an irradiation intensity of UV-A by 6, 18, and 30 W L^{-1}, respectively. When the $Ag/TiO_2/Fe_3O_4$ loading was varied for each value of the initial 4-CP concentration, all other experimental conditions were kept constant. Fig. 5(a) shows the initial 4-CP concentration effects that an increased concentration lead to a decrease of the degradation rate. Fig. 5(b) shows that a dosage of 0.7 g L^{-1} is worse than one of 0.5 g L^{-1}; a reduction in reaction rate was generally observed at photocatalyst overdose, due to the opacity caused by excess photocatalyst clusters. Fig. 5(c) shows that when the intensity is at its strongest, there is enhancement in 4-CP degradation. It can be concluded that the optimum amount of photocatalyst is dependent on the concentration of the substrate. The optimal condition for 4-CP decomposition would

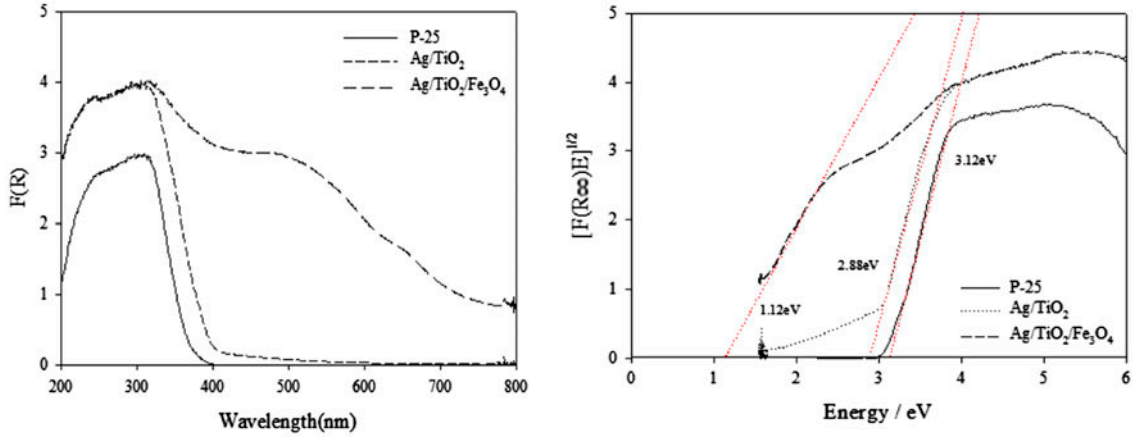

Fig. 3. Diffuse reflectance spectra of TiO_2, Ag/TiO_2, and $Ag/TiO_2/Fe_3O_4$.

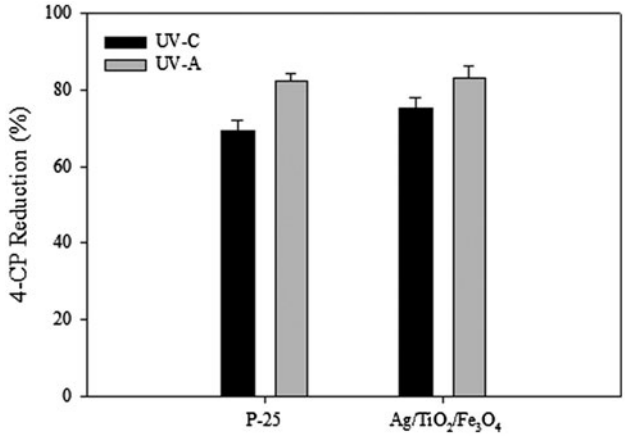

Fig. 4. Photocatalytic activity of $Ag/TiO_2/Fe_3O_4$ for 4-CP degradation under UV-C and UV-A irradiation.

therefore correspond to $0.5\,g\,L^{-1}$ of $Ag/TiO_2/Fe_3O_4$, $77.8\,\mu mol\,L^{-1}$ of 4-CP, and 30 W of UV-A since the highest removal rate was obtained at these values. The slope of Fig. 5(d) shows the apparent first-order rate that Degussa P25 TiO_2, Ag/TiO_2, and $Ag/TiO_2/Fe_3O_4$ each promotes, and are 2.1×10^{-3}, 2.8×10^{-3}, and $5.1\times10^{-3}\,min^{-1}$, respectively (Table 1). It can be seen from the values that the kinetic rate constant for the $Ag/TiO_2/Fe_3O_4$ is six times as high as that for Degussa P25 TiO_2 and Ag/TiO_2.

The rate of the photocatalytic degradation of 4-CP is a function of the initial concentration of 4-CP. This rate can be evaluated with the adsorption reaction rate constant ($k_{adsorption}$), photocatalytic reaction rate constant ($k_{photocatalytic}$), and adsorption coefficient ($k_{adsorption+photocatalytic}$) initial concentration of 4-CP by the inverse of *Langmuir–Hinshelwood* equation:

$$-dt/d[4-CP] = 1/k_{adsorption} + 1/\{k_{adsorption}\,k_{photocatalysis}[4-CP]\}$$

$$-dt/d[4-CP] = 1/k_{adsorption} + 1/\{k_{adsorption}\,k_{photocatalysis}[4-CP]\}$$

A plot of the inverse of the initial rate of 4-CP photodegradation obtained as a function of the reciprocal initial 4-CP concentration is shown in Fig. 6. The values of $k_{adsorption}$ and $k_{photocatalysis}$ can be derived from the intercept and the slope of these straight lines. The adsorption of 4-CP on a semiconductor catalyst is a crucial factor in the kinetics of heterogeneous photodegradation. The photocatalysis of 4-CP on the $Ag/TiO_2/Fe_3O_4$ composite was obtained as $k_{photocatalytic}=2.86\times10^{3}$, $k_{adsorption}=0.5\times10^{-4}$ by optimal conditions (Table 2).

3.2. Test of cyclic usage of $Ag/TiO_2/Fe_3O_4$

In order to determine whether the cyclic usage was possible for the $Ag/TiO_2/Fe_3O_4$ photocatalyst, the photocatalytic degradation experiments of 4-CP were repeated for four cycles. The change in residual concentrations of 4-CP under cycling conditions is shown in Fig. 7. It was observed that 4-CP was degraded rapidly by the present photocatalyst under UV irradiation. The photocatalytic activity of the present photocatalyst was slightly reduced in stirred aqueous solution, and the photocatalytic activity of $Ag/TiO_2/Fe_3O_4$ remained at about 83% of its activity as prepared after being used four times; the degradation percentage of 4-CP can reach 70% when the irradiation time is 5 h. Thus the findings suggested that the

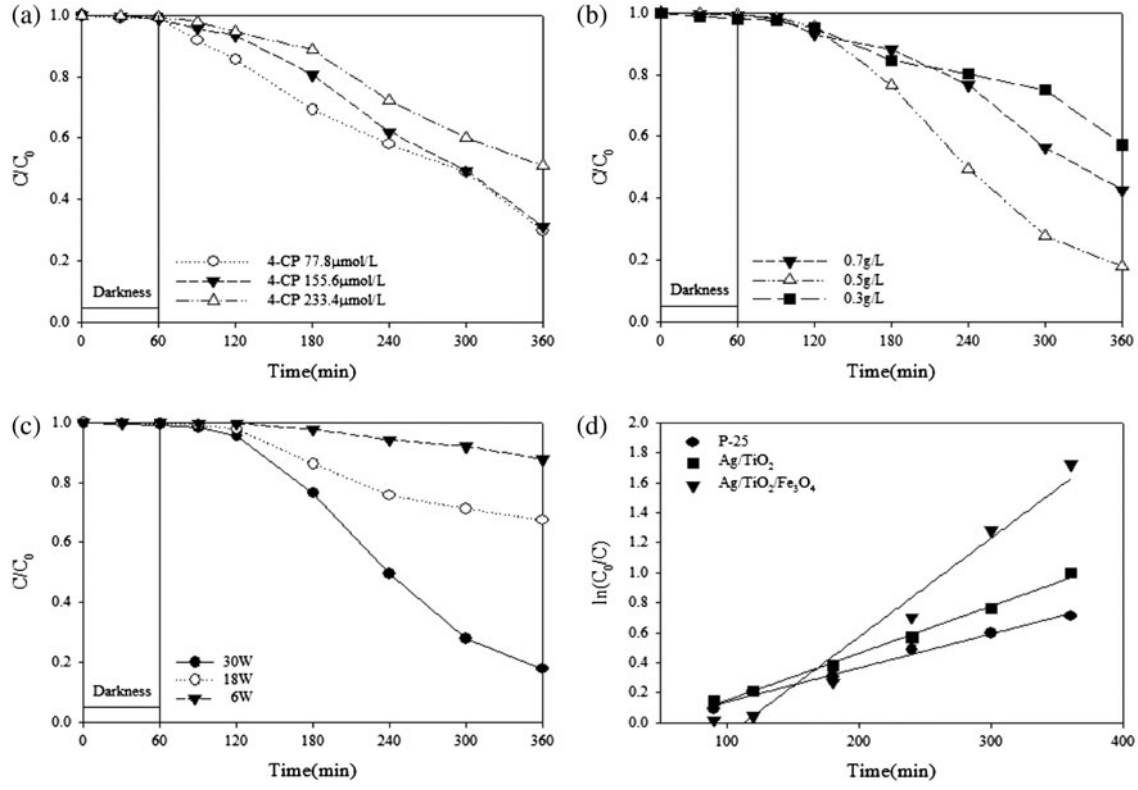

Fig. 5. Photocatalytic activity of $Ag/TiO_2/Fe_3O_4$ for: (a) initial concentration of 4-CP; (b) dosage of $Ag/TiO_2/Fe_3O_4$; (c) irradiation intensity; (d) first-order plots of 155.5 μM 4-CP degradation by different catalysts (TiO_2, Ag/TiO_2, and $Ag/TiO_2/Fe_3O_4$).

Table 1
First-order plots of 4-CP degradation with different catalysts

Catalysts	K	R^2
Degussa P25 TiO_2	0.0023	0.9913
Ag/TiO_2	0.0031	0.9949
$Ag/TiO_2/Fe_3O_4$	0.0066	0.9644

deposited anatase TiO_2 was firmly attached to the Fe_3O_4 surface, and cannot be easily exfoliated from Fe_3O_4 in mechanically stirred solutions for long periods. Simultaneously, it also proves that the final removal of 4-CP from solution is caused by the photocatalytic degradation other than the adsorption process that will lead to saturated adsorption of 4-CP on the photocatalyst. These results indicate that cyclic usage of the $Ag/TiO_2/Fe_3O_4$ composite is possible, and its potential stability in treating polluted water is satisfactory; it can therefore be potentially employed in continuous photocatalytic degradation processes.

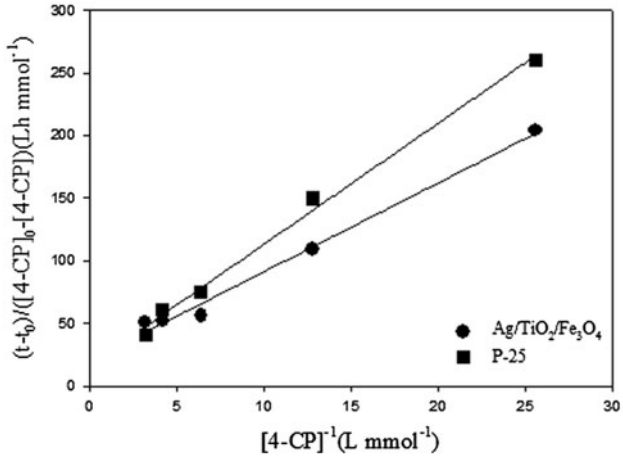

Fig. 6. *Langmuir-Hinshelwood* kinetics for the photocatalytic degradation of 4-CP using Degussa P25 TiO_2 and $Ag/TiO_2/Fe_3O_4$. (0.5 g L^{-1} of $Ag/TiO_2/Fe_3O_4$, 77.8 μmol L^{-1} of 4-CP, and 30 W of UV-A).

Table 2
Apparent reaction rate constant and adsorption constant

Catalysts	$k_{adsorption+photocatalytic}$	$k_{adsorption}$	$k_{photocatalytic}$	R^2
Degussa P25 TiO_2	0.10	0.6×10^{-4}	1.73×10^{3}	0.9913
$Ag/TiO_2/Fe_3O_4$	0.14	0.5×10^{-4}	2.86×10^{3}	0.9902

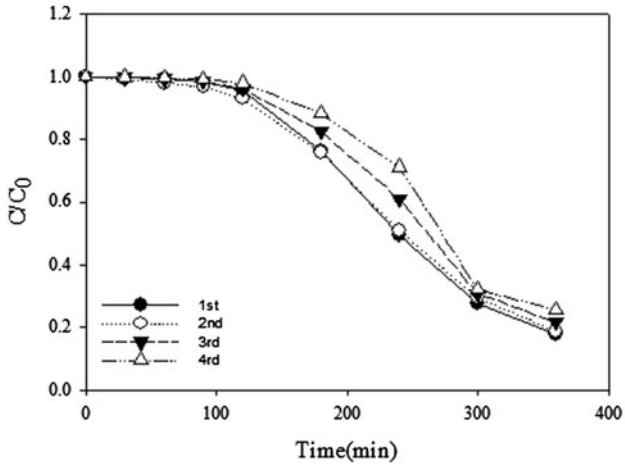

Fig. 7. The cyclic performance of $Ag/TiO_2/Fe_3O_4$.

4. Conclusion

In this study, a composite $Ag/TiO_2/Fe_3O_4$ catalyst was successfully synthesized. The photocatalytic activities of Degussa P25TiO_2, Ag/TiO_2, and $Ag/TiO_2/Fe_3O_4$ towards 4-CP degradation under UV-A irradiation were compared. From the results obtained, we can conclude that the photocatalytic activity under UV irradiation of $Ag/TiO_2/Fe_3O_4$ was higher than that of both Degussa P25 TiO_2 and Ag/TiO_2; the 4-CP was degraded 82, 51, and 64% by $Ag/TiO_2/Fe_3O_4$, Degussa P25 TiO_2, and Ag/TiO_2, respectively. The effect of $Ag/TiO_2/Fe_3O_4$ loading on three on decomposition rate factors was studied. The photocatalytic degradation rate of 4-CP was affected by initial concentration, dose, and irradiation intensity. The proper conditions were identified as 77.8 μmol L^{-1}, 0.5 g L^{-1}, and 30 W, respectively.

The first-order rate constants for the synthesized Degussa P25 TiO_2, Ag/TiO_2, and $Ag/TiO_2/Fe_3O_4$ are 2.1×10^{-3}, 2.8×10^{-3}, and 5.1×10^{-3} min^{-1}, respectively. The reaction rate of $Ag/TiO_2/Fe_3O_4$ was faster than both Degussa P25 TiO_2 and Ag/TiO_2.

The photocatalysis of 4-CP on the $Ag/TiO_2/Fe_3O_4$ was obtained as $k_{photocatalytic} = 2.86 \times 10^3$, $k_{adsorption} = 0.5 \times 10^{-4}$ as 77.8 μmol L^{-1}, 0.5 g L^{-1}, and 30 W, respectively.

The photocatalytic activity of $Ag/TiO_2/Fe_3O_4$ remains at about 83% of its activity as prepared after being used four times, and the degradation percentage of 4-CP can reach 70% when irradiation time is 5 h. The photocatalytic activity of $Ag/TiO_2/Fe_3O_4$ was enhanced compared to Degussa P25 TiO_2 and Ag/TiO_2 extension of wavelength.

The cyclic usage of $Ag/TiO_2/Fe_3O_4$ composite was determined as satisfactory for its application in the treatment of water pollution. The recovery of $Ag/TiO_2/Fe_3O_4$ was demonstrated to be possible.

Acknowledgment

This subject was supported by the Korea Ministry of Environment as "Global Top Project" (Project No.: GT-11-B-01-013-0).

References

[1] L. Calvo, A.F. Mohedano, J.A. Casas, M.A. Gilarranz, J.J. Rodriguez, Treatment of chlorophenols bearing wastewaters through hydrodechlorination using Pd/activated carbon catalysts, Carbon 42 (2004) 1371–1375.
[2] A. Bhunia, S. Durani, P.P. Wangikar, Horseradish peroxidase catalyzed degradation of industrially important dyes, Biotechnol. Bioeng. 72(5) (2001) 562–567.
[3] M. Wagner, J.A. Nicell, Treatment of a foul condensate from kraft pulping with horseradish peroxidase and hydrogen peroxide, Water Res. 35(2) (2001) 485–495.
[4] N.K. Sahoo, K. Pakshirajan, P.K. Ghosh, A. Ghosh, Biodegradation of 4-cholorophenol by Arthrobacter chlorophenolicus A6: Effect of culture conditions and degradation kinetics, Biodegradation 22 (2011) 2755.
[5] J.A. Zazo, J.A. Casas, A.F. Mohedano, M.A. Gilarranz, J.J. Rodriguez, Chemical pathway and kinetics of phenol oxidation by Fenton's reagent, Environ. Sci. Technol. 39 (2005) 9295–9302.
[6] S. Lathasree, A. Nageswara Rao, B. SivaSankar, V. Sadasivam, K. Rengaraj, Heterogeneous photocatalytic mineralisation of phenols in aqueous solutions, J. Mol. Catal. A: Chem. 223(1–2) (2004) 101–105.
[7] J. Wang, W. Sun, Z. Zhang, Z. Jiang, X. Wang, R. Xu, R. Li, X. Zhang, Preparation of Fe-doped mixed crystal TiO_2 catalyst and investigation of its sonocatalytic activity during degradation of azo fuchsine under ultrasonic irradiation, J. Colloid Interface Sci. 320(1) (2008) 202–209.

[8] A. Fujishima, K. Honda, Electrochemical photolysis of water at a semiconductor electrode, Nature 238 (1972) 37–38.
[9] X. Yu, S. Liu, J. Yu, Superparamagnetic γ-Fe_2O_3@-SiO_2@TiO_2 composite microspheres with superior photocatalytic properties, Appl. Catal., B 104 (2011) 12–20.
[10] L. Chengzhu, S. Wendong, Z. Yujiang, L. Chengzhan, C. Ying, PVP-assisted synthesis and visible light catalytic property of Ag/AgBr/TiO_2 ternary nanostructure, J. Alloys Compd. 581 (2013) 115–120.
[11] P. Wang, B. Huang, X. Zhang, X. Qin, H. Jin, Y. Dai, Z. Wang, J. Wei, J. Zhan, S. Wang, Synthesis of highly efficient Ag@AgCl plasmonic photocatalysts with various structures, Chem. Eur. J. 15(8) (2009) 1821–1824.
[12] H.Y. Wen, L.X. Zi, L. Li, Synthesis and photocatalytic properties of core-shell TiO_2@$ZnIn_2S_4$ photocatalyst, Chin. Chem. Lett. 24 (2013) 984–986.
[13] Q. Shi, D. Yang, Z.Y. Jiang, J. Li, Visible-light photocatalytic regeneration of NADH using P-doped TiO_2 nanoparticles, J. Mol. Catal. B: Enzym. 43 (2006) 44–48.
[14] C.T. Yavuz, J.T. Mayo, W.W. Yu, A. Prakash, J.C. Falkner, S. Yean, L. Cong, H.J. Shipley, A. Kan, M. Tomson, D. Natelson, V.L. Colvin, Low-field magnetic separation of monodisperse Fe_3O_4 nanocrystals, Science 314 (2006) 964–967.
[15] T. Zhang, X. Zhang, J. Ng, H. Yang, J. Liu, D.D. Sun, Fabrication of magnetic cryptomelane-type manganese oxide nanowires for water treatment, Chem. Commun. 47 (2011) 1890–1892.
[16] X. Song, L. Gao, Facile synthesis of polycrystalline NiO nanorods assisted by microwave heating, J. Am. Ceram. Soc. 91 (2008) 3465–3468.
[17] C. Wang, C. Böttcher, D.W. Bahnemann, J.K. Dohrmann, *In situ* electron microscopy investigation of Fe(III)-doped TiO_2 nanoparticles in an aqueous environment, J. Nanopart. Res. 6 (2004) 119–122.
[18] Z. Liu, X. Zhang, T. Murakami, A. Fujishima, Sol–gel SiO_2/TiO_2 bilayer films with self-cleaning and antireflection properties, Sol. Energy Mater. Sol. Cells 92(11) (2008) 1434–1438.
[19] B. Sun, E.P. Reddy, P.G. Smirniotis, Effect of the Cr^{6+} concentration in Cr-incorporated TiO_2-loaded MCM-41 catalysts for visible light photocatalysis, Appl. Catal., B 57 (2005) 139–149.
[20] M.R. Hoffmann, S.T. Martin, W. Choi, D. Bahnemann, Environmental applications of semi-conductor photocatalysis, Chem. Rev. 95 (1995) 69–96.